

Analysis and Comparison of Results of Thermomechanical Phenomena in the Cutting of Steel C45 and Titanium Alloy Ti6Al4V by Finite Element Method

Thanh Hung Dao¹

¹University of Technology and Education - The University of Danang,
48 Cao Thang Street, Hai Chau District, Da Nang city, Viet Nam

Abstract: This article presents predictions and comparisons of simulation results of the distribution of the effective stress in the cutting area, the distribution of heat in the cutting area and on the front surface of the cutting tool, the change in cutting force on the cutting tool in cutting two materials: Steel C45 and titanium alloy Ti-6Al-4V. The material of the cutting tool is WC-Co carbide. The orthogonal cutting model is created by the finite element method in the environment of Deform 3D V6.1. The thermal properties of materials in the model are functions of temperature. Based on the results obtained from the simulations, the maximum temperature on the chips and on the front surface of the cutting tool is determined and compared. Performing evaluations for the distribution of effective stress in the cutting area, the change in cutting force. The results of the article show that the working condition of the cutting tool in cutting titanium alloy Ti-6Al-4V is harder than the case of cutting Steel C45 in the same cutting mode. The elastic deformation of all elements of the technological system in cutting titanium alloy Ti-6Al-4V is greater than the case of cutting steel C45. These results show that it is necessary to choose a rational cutting mode, a rational cooling system, high rigidity of the technological system in cutting the titanium alloy Ti-6Al-4V in actual production conditions.

Keywords: Cutting heat, simulation, cutting force, effective stress in cutting area.

1. Introduction

Metal cutting is a complex process in which elastic deformation and plastic deformation occur. Metal cutting occurs in high friction, with heat, with shrinkage of the chips, with changes in physical and mechanical properties on the surface of the machined part, with the wear of the cutting tool. All of these affect the performance of the manufacturing process [1] [2].

The study of the physical and mechanical phenomena that occur during the processing of metals by cutting allows us to clearly understand the causes and consequences of these phenomena. Prediction of the effects of physical and mechanical elements on the cutting tool, on the surface of the machined part, on the productivity of manufacturing process. Hence, it is easy to control the process of metal cutting through the selection of rational cutting modes to ensure the quality of the surfaces of the machined part and high economic efficiency.

There are many studies that study the thermomechanical phenomena during the cutting process, but only for one material of the workpiece, there is no comparison or assessment of the differences in thermomechanical phenomena when cutting different materials of the workpiece in one cutting mode. In several of them, the thermomechanical parameters of the workpiece materials are used in constant values [3] [4], according to which the correctness of the simulation results is affected.

In this article, the orthogonal model of metal cutting is created by the finite element method in Solidworks 2018 and Deform 3D V6.1. The simulation process is carried out with a workpiece, the materials of which are steel C45 and titanium alloy Ti-6Al-4V with thermo-mechanical properties are functions of temperature. Based on the simulation results, the distribution of heat and effective stresses in the cutting area are considered. Determination and comparison of the highest temperature on the chips and on the cutting tool, determination and comparison of the average values of the effective force on the cutting tool during metal processing by cutting with two different workpiece materials.

2. The Main Theory and Method of Research

The heat generated during metal cutting is generated from deformation and friction. This friction exists in the contacts on the front surface of the cutting tool with the chips, and on the rear surface of the cutting tool with the machined surface of the part. Deformations during metal cutting are elastic and plastic in the cutting area. The amount of heat generated during cutting in a minute is determined by the formula (1) [1] [2]:

$$Q = \frac{P_z \cdot v}{E} = Q_{bd} + Q_{ms} \text{ [Kcal / min]} \quad (1)$$

In the above formula, P_z : The main constituent force in unit [KG], v : Cutting speed in unit [m/min], $E = 427$ [KGm/Kcal]: mechanical equivalent of heat, Q_{bd} : heat generated due to deformation, Q_{ms} : heat generated during cutting due to the contact areas between the cutting tool with the chips and the machined surface.

The heat generated during cutting is distributed in the chips (50% ÷ 86%), in the cutting tool (40% ÷ 10%), in the machined part (9% ÷ 3%), in the environment (1%) [1] [2].

The heat generated during cutting greatly affects the cutting process.

The heat generated during cutting affects the accuracy of the machined part according to the formula (2):

$$d_{th} = D - 2h_2 = D - 2h - \Delta D - 2\Delta L_d \quad (2)$$

In the formula (2), d_{th} is actual diameter of the machined part, D is nominal diameter of the part, h is initial machining allowance, h_2 is machining allowance corresponding to an increase in the diameter of the machined part due to heat generation during cutting, ΔD is the change in the diameter of the workpiece due to heat during cutting, ΔL_d is the change in the length of the cutting tool due to heat during cutting. Therefore, according to the formula (2), the actual diameter of the machined part will lose accuracy due to heat generation during cutting. The heat generated during cutting affects the quality on the machined surface of the part and changes the physical and mechanical properties of the machined surface of the part. Due to sharp changes in temperature on the workpiece surface with changes in cutting force, the consequence of which are residual stresses, microcracks, microroughness created on the machined surfaces of the part. The machined surfaces of the part will be hardened. The heat generated during cutting greatly affects the performance of the cutting tool, changes the physical and mechanical properties of the cutting tool, reduces the wear resistance and hardness of the cutting tool, and increases the wear of the cutting tool. Thus, heat during cutting strongly affects the cutting process, therefore, it is necessary to determine its values and the relationship between heat during cutting with stresses in the cutting area. To evaluate the levels of influence of heat during cutting on the cutting process, it is necessary to determine the temperature in the cutting area [1] [2].

3. Creating an Orthogonal Model of Metal Cutting

Currently, there are many programs for simulating the cutting model, specifically: ANSYS, ABAQUS, DEFORM 3D, LS DYNA, ... In this article, the simulation and analysis of the cutting model are performed in the Deform-3D v6.1 environment [5]. The constituent components of the cutting model were created in Solid works 2018. The cutting model is orthogonal, as in Figure 1. The cutting model consists of a workpiece and a cutting tool. The dimensions of the workpiece and cutting tool are presented in Table 1.

3.1. Thermomechanical properties of materials of the cutting model

The thermomechanical properties of materials change with the influence of temperature [6]. Therefore, if these thermomechanical properties are used as constant values, then the accuracy of the simulation results will not be good. In this article, the thermomechanical properties of materials are used as functions of temperature. Steel C45 is a popular material in the general engineering industry. The thermomechanical properties of steel C45 are presented in table 2 [6] [7]. The titanium alloy Ti-6Al-4V is a good material, which is better than ordinary steels, specifically: its density is equal to half relative to steel, high strength [8]. Titanium alloy is used in the aviation and space industries and in medicine [9]. The thermomechanical properties of the titanium alloy Ti-6Al-4V are presented in Table 3 [8]. The cutting tool of the cutting model is a WC-Co hard alloy with thermomechanical properties presented in Table 4 [8] [10].



Figure 1. Orthogonal cutting model

Table 1: The geometry parameters of the workpiece and cutting tool.

Workpiece	Cutting tool
Length: 100mm	Rake angle: 5°
Height: 50mm	Back corner: 5°
Width: 5mm	Cutting edge rounding radius: 0.015mm

Table 2: Thermomechanical properties of steel C45 [6] [7]

The material of the workpiece	C45
Density (g/cm ³)	7.87
Modulus of elasticity (MPa)	250.29 – 0.1086 × T
Poisson's ratio	0.3
Heat capacity (N/mm ² ·C-1)	3.518 + 6.37 × 10 ⁻⁴ × T + 0.39 × 10 ⁻⁵ × T ²
Thermal conductivity (W/m·C-1)	51.638 – 0.0228 × T
Thermal expansion coefficient (mm·mm-1·C-1)	8.8608 + 0.0068 × T
Melting temperature (°C)	1460 °C

Table 3: Thermomechanical properties of titanium alloy Ti-6Al-4V [8].

The material of the workpiece	Ti-6Al-4V
Density (g/cm ³)	4.43
Modulus of elasticity (MPa)	0.7412 × T + 113.375
Poisson's ratio	0.31
Heat capacity (N/mm ² ·C-1)	2.24 × 10 ^{0.0007 × T}
Thermal conductivity (W/m·C-1)	7.039 × 10 ^{0.0011 × T}
Thermal expansion coefficient (mm·mm-1·C-1)	3.1 × 10 ⁻⁹ × T + 7.1 × 10 ⁻⁶
Melting temperature (°C)	1660 °C

Table 4: Thermomechanical properties of the WC-Co carbide [8] [10].

The material of the cutting tool.	WC-Co
Density (g/cm ³)	15.63
Modulus of elasticity (MPa)	500
Poisson's ratio	0.25
Heat capacity (N/mm ² ·C-1)	0.0005 × T + 2.07
Thermal conductivity (W/m·C-1)	0.042 × T + 36
Thermal expansion coefficient (mm·mm-1·C-1)	4.7 × 10 ⁻⁶
Melting temperature (°C)	2870 °C

3.2. The Johnson-Cook material model

In this article, the Johnson-Cook material model is used to simulate the process of metal cutting. The Johnson-Cook material model combines the effects of equivalent strain, strain rate, and temperature. The Johnson-Cook material model is popularly used in simulation of metal cutting under conditions of high deformation, high speed of deformation and high temperature [4]. In comparisons of the simulation results for metal cutting, the Johnson-Cook material model with the Power law material model give deviations of the simulation results less than the Litonski-Batra, Bodner-Partom models, relative to the experimental results [11]. The Johnson-Cook material model is represented as in equation (3) [11]:

$$\bar{\sigma} = \left[A + B \times (\bar{\epsilon})^n \right] \left[1 + C \times \ln \left(\frac{\dot{\bar{\epsilon}}}{\dot{\bar{\epsilon}}_0} \right) \right] \left[1 - \left(\frac{T - T_0}{T_m - T_0} \right)^m \right] \quad (3)$$

In equation (3), it represents that many elements affect the stress of any material: equivalent deformation, strain rate, heat release during cutting processing. A is the yield strength under slow loading at room temperature, B is the material hardening modulus, C is the coefficient of sensitivity to the strain rate, $\bar{\epsilon}$ is the equivalent strain, $\dot{\bar{\epsilon}}$ is the strain rate, $\dot{\bar{\epsilon}}_0$ is the reference strain rate, m is the coefficient of thermal compaction; n is the solidification coefficient, T_0 is the room temperature, T_m is the melting point. The parameters of the Johnson-Cook material model for Steel C45 and the titanium alloy Ti-6AL-4V are presented in Table 5. Due to steel C45, it is equivalent to AISI 1045 steel, therefore, the parameters of AISI 1045 steel in

the Johnson-Cook material model can be used for steel C45 [7] [12] [13].

Table 5: The parameters of the Johnson-Cook material model for steel C45 and the titanium alloy Ti-6Al-4V [6] [14] [15].

Materials	T_m	T_0	A	B	C	n	m
C45	1460	20	553.1	600.8	0.0134	0.234	1
Ti-6Al-4V	1660	20	782.7	498.4	0.028	0.28	1

3.3. Creating a finite element simulation model

At the beginning, the geometry of the workpiece and cutting tool is built in Solidworks 2018 with the dimensions in Table 1. After creating three-dimensional models of the workpiece and cutting tool in Solidworks 2018, an orthogonal cutting model was created in the Deform-3D V6.1 environment, which includes two objects: a workpiece and a cutting tool. The meshing of the finite elements for the workpiece and the cutting tool is performed according to the parameters in Table 6.

Table 6: Parameters for the mesh of the finite element model.

Parameters for the grid	Workpiece	Cutting tool
Type of elements	Tetrahedral	Tetrahedral
Number of elements	103365	13667

In the finite element method, if the number of elements increases, the accuracy of the results will increase, but the calculation time will increase significantly [5].

3.4. The boundary conditions of the orthogonal cutting model

The boundary conditions of the orthogonal cutting model are presented in Figure 2.

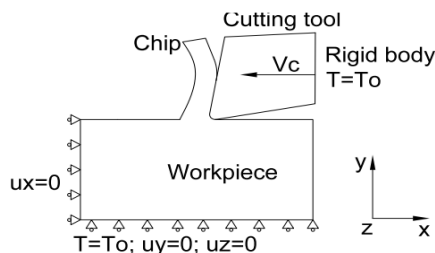


Figure 2. The boundary conditions of the orthogonal cutting model.

Figure 2 shows that the degrees of freedom of movement of the workpiece from the axes OX, OY, OZ are deprived. The cutting tool moves along the OX axis with a cutting speed of $V_c = 70\text{m/min}$, which is selected based on the durability of the material of the cutting tool [16]. Cutting thickness: $a=1\text{mm}$, cutting width: $b=5\text{mm}$. During the simulation, the cutting tool is considered a rigid body [12]. The initial temperature is used for the workpiece and cutting tool $T_0=20^\circ\text{C}$. The friction between the workpiece and the cutting tool is expressed on the basis of the Coulomb's theory as in these equations:

$$\begin{cases} \tau_f = \tau_{\max} & \text{if } \mu \cdot \sigma_n \geq \tau_{\max} \\ \tau_f = \mu \cdot \sigma_n & \text{if } \mu \cdot \sigma_n < \tau_{\max} \end{cases} \quad (4)$$

In the equations (4), τ_f is the shear stress in the contact plane, τ_{\max} is the maximum shear stress of workpiece material, σ_n is the normal stress, μ is the coefficient of friction. The value of the coefficient of friction for the simulation is 0.4.

3.5. The basis of the theory for the analysis of cutting forces in the orthogonal cutting model [1] [2]

The resulting cutting force is the sum of the component forces along the loaded planes as in Figure 3.

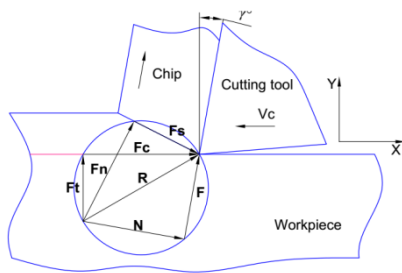


Figure 3. Analysis of cutting forces in the orthogonal cutting plane.

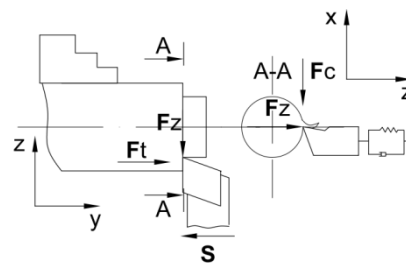


Figure 4. Radial component force Fz in longitudinal turning [17].

Figure 3 shows that the main component is the force F_c , whose direction along the axis OX. As a result of the simulation, F_c is F_x . The feed force F_t has a direction along the axis OY. As a result of the simulation, F_t is F_y . All of these are the basis on which the constituent forces of the simulation results are determined.

In addition to the two component forces F_c and F_t , there is also the component force F_z , whose direction along the axis OZ. This component force F_z is obtained in simulation with three-dimensional model. In longitudinal turning, the component force F_z has a direction along the holder of the cutting tool, called the radial component force as in Figure 4 [17]. The component force F_z strongly affects the elastic deformation of all elements of the technological system in cutting, in which the workpiece is considered a rigid body according to the formula (5) [18]:

$$y = \frac{F_z}{J} \quad (5)$$

In the formula (5), J is the rigidity of the technological system [kN/m]; F_z is the radial component of the cutting force; y is the displacement of the cutter head in the direction of the force F_z due to elastic deformation [mm]. The rigidity of each element of the technological system is a certain value as in the formula (5). Due to the movement of the cutter head in the direction of the radial cutting force F_z , the deviation of the diameter and the deviation of the geometric shapes of the machined part are caused and the surface quality of the machined part deteriorates. From the formula (5), the elastic deformation of each element of the technological system is determined [18]:

$$y_{bd} = \frac{F_z}{J_{bd}}; y_{ut} = \frac{F_z}{J_{ut}}; y_{us} = \frac{F_z}{J_{us}} \quad (6)$$

The elastic deformation of all elements of the technological system is determined by:

$$y_{ht} = y_{bd} + y_{ut} + y_{us} \quad (7)$$

In the formulas (6) and (7): are the elastic deformations of the lathe carriage, front headstock, tailstock, and technological system, respectively. are respectively the rigidity of the lathe carriage, front headstock, tailstock. According to the formulas (5), (6), (7), after obtaining the simulation results based on the radial component of the force F_z through displacements of the cutter head due to elastic deformations of each element in the technological system, the deviation of the diameter and quality of the machined surfaces of the part will be evaluated [17] [18].

4. Simulation Results and Discussion

Run the calculation for the finite element model that describes the processing of metals by cutting with the given: cutting speed $V_c=70\text{m/min}$, cutting thickness $a=1\text{mm}$, cutting width $b=5\text{mm}$, the number of simulation steps is 500. The heat transfer coefficient is used in the simulation: $h=1000\text{kW/m}^2\cdot\text{C}^{-1}$ [19]. The workpiece material in the simulation is respectively Steel C45 and titanium alloy Ti-6Al-4V.

4.1. Simulation results with the workpiece material C45

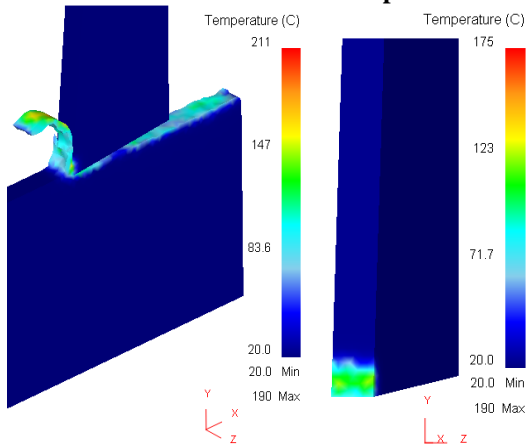


Figure 5. Heat generated in the cutting and on the front surface of the cutting tool.

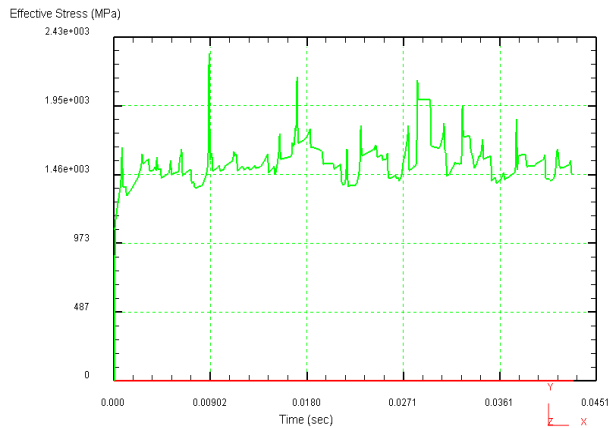


Figure 6. Graph of effective stress in the cutting area.

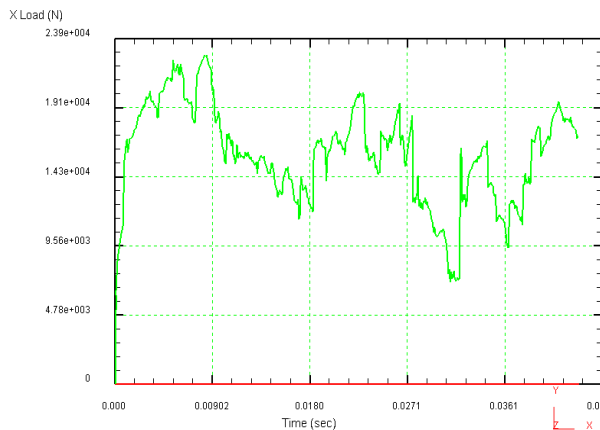


Figure 7. The main constituent force is Fx (N).

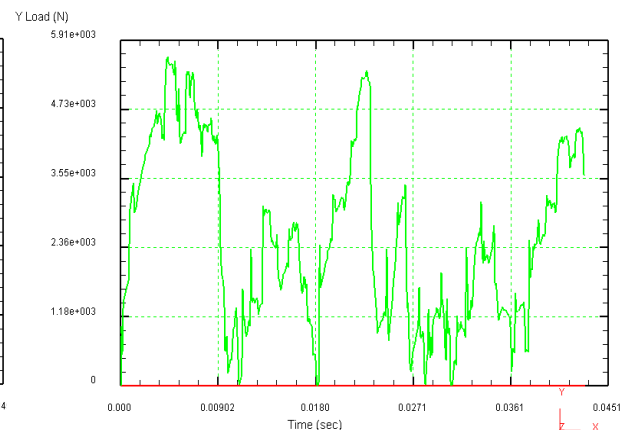


Figure 8. The feed force Fy (N).

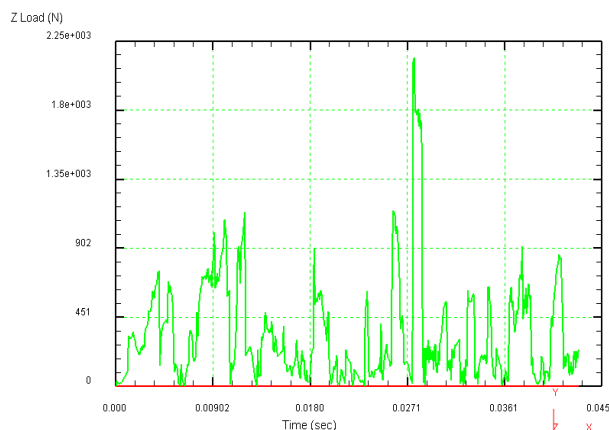


Figure 9. The radial component force Fz (N).

Figure 5 shows the distribution of heat generated in cutting in the workpiece, on the chips and on the cutting tool. The maximum temperature is on the chips in contact with the front surface of the cutting tool $T = 211^{\circ}\text{C}$. Figure 5 also shows the distribution of heat on the cutting tool when machining Steel C45. The heat of cutting is distributed on the front surface of the cutting tool due to sliding chips on the front surface of the cutting tool and the transfer of heat from the chips to the cutting tool. The maximum temperature on the front surface of the cutting tool $T=175^{\circ}\text{C}$. Figure 6 shows a graph of the effective stress in the cutting area. The

effective stress increases rapidly from the beginning of cutting, then oscillates in the region from 1.31×10^3 MPa to 2.32×10^3 MPa. The main constituent force is shown in Figure 7. The value of the main component of the cutting force increases rapidly from the beginning of cutting $t = 0$ (s), then oscillates to $t = 0,043$ (s). The value of the main component of the force oscillates due to the mechanical behavior of the workpiece material. Under the action of an external force, elastic deformation and plastic deformation occur in metals. After that, the metal is destroyed. The value of the external force slowly increases from the point of plastic deformation to the point of fracture, then slowly decreases. The processes of deformation, fracture of the metal and the formation of chips occurs continuously during the processing of metals by cutting, so the value of the main cutting force oscillates in the region from 7.06×10^3 (N) to 2.27×10^4 (N). The average value of the main component of the cutting force is 1.58×10^4 (N). Figure 8 shows the feed force F_y (N), the average value of which is 2.5×10^3 (N). Figure 9 shows the radial component force F_z .

4.2. Simulation results with the workpiece material Ti-6Al-4V

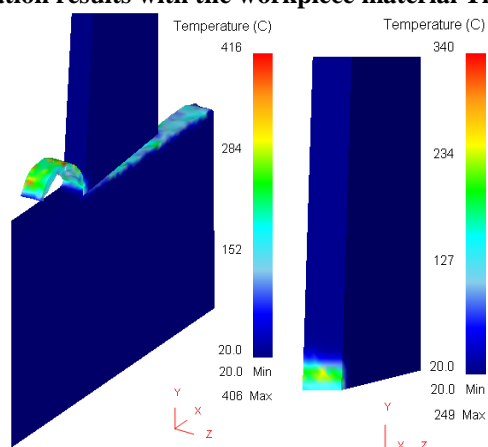


Figure 10. Heat generated in the cutting area and on the front surface of the cutting tool.

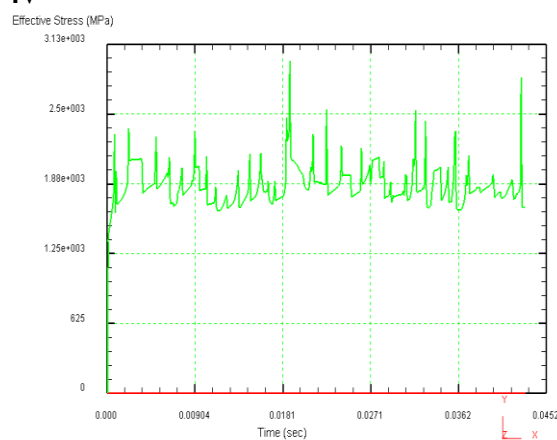


Figure 11. Graph of effective stress in the cutting area.

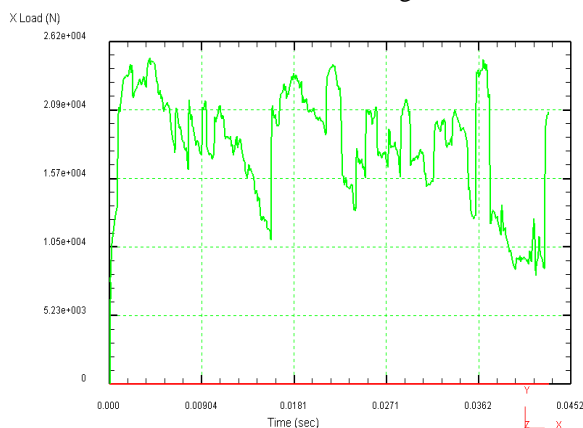


Figure 12. The main constituent force is F_x (N).

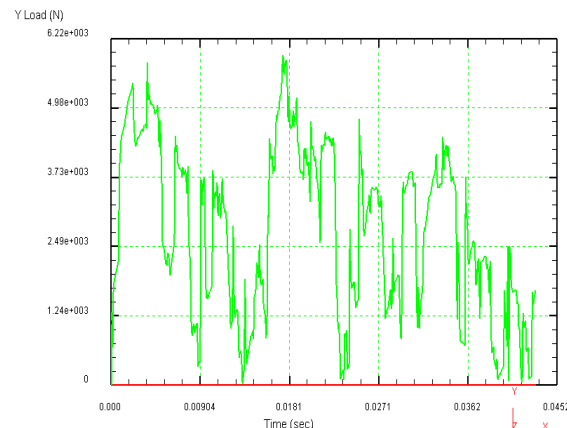


Figure 13. The feed force F_y (N).

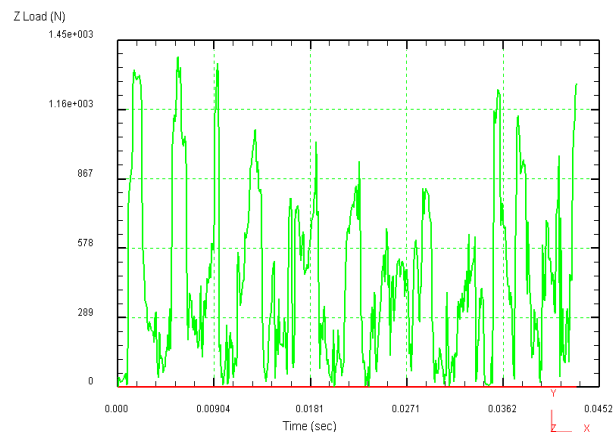


Figure 14. The radial component force F_z (N).

Figure 10 shows the distribution of heat generated in cutting in the workpiece, on the chips and on the cutting tool. The maximum temperature is on the chips in contact with the front surface of the cutting tool $T=416^{\circ}\text{C}$. Figure 10 also shows the distribution of heat generated during cutting on a cutting tool in the case of cutting with Ti-6Al-4V. The heat of cutting is distributed on the front surface of the cutting tool due to the sliding chips on which. In addition, heat is transferred from the chips to the cutting tool, the maximum temperature on the cutting tool is $T=340^{\circ}\text{C}$. Figure 11 shows a graph of the effective stress in the cutting area, which increases rapidly from the beginning of cutting and then it oscillates in the region from 1.61×10^3 MPa to 2.98×10^3 MPa. The oscillation region of the effective stresses in the cutting of the titanium alloy Ti-6Al-4V is wider than the case of cutting steel C45. The main component of the cutting force is shown in Figures 12. The value of the main component of the cutting force increases rapidly from the beginning $t=0$ (s) and continuously oscillates until the end of the simulation $t=0,043$ (s). The average value of the main component of the force is 1.82×10^4 (N) and the region of oscillation of the main component of the cutting force is from 8.32×10^3 (N) to 2.49×10^4 (N). In Figure 13, the feed force is shown, the average value of which is 2.75×10^3 (N). Figure 14 shows the radial component force F_z .

4.3. Comparison of simulation results of thermomechanical phenomena in cases of cutting steel C45 and titanium alloy Ti-6Al-4V

Table 7: The results of simulation of thermomechanical phenomena in cases of cutting steel C45 and titanium alloy Ti-6Al-4V

Workpiece material	Steel C45	Ti-6Al-4V
The maximum temperature on the chips during metal cutting.	211°C	416°C
The maximum temperature on the front surface of the cutting tool.	175°C	340°C
The average value of the main component of the force. (N)	1.58×10^4	1.82×10^4
The average value of the feed force component. (N)	2.5×10^3	2.75×10^3
The average value of the radial force component. (N)	340.45	443.20
Oscillation width of effective stress in cutting area. (Mpa)	$1.31 \times 10^3 \div 2.32 \times 10^3$	$1.61 \times 10^3 \div 2.98 \times 10^3$

Table 7 shows the differences in the results of simulations of thermomechanical phenomena when cutting steel C45 and titanium alloy Ti-6Al-4V. Specifically, large heat is distributed on the chips in the case of cutting the titanium alloy Ti-6Al-4V, the maximum temperature on the chips $T=416^{\circ}\text{C}$ and the maximum temperature on the front surface of the cutting tool $T=340^{\circ}\text{C}$. The heat in cutting titanium alloy Ti-6Al-4V is much greater than the case of cutting Steel C45 because of the thermal conductivity of titanium alloy Ti-6Al-4V is much less than Steel C45. In addition, the strength of the titanium alloy Ti-6Al-4V is high, therefore, it requires a lot of cutting work which is converted into heat of cutting. Table 7 also shows the average value of

the main component of the cutting force in cutting the titanium alloy Ti-6Al-4V is much larger than the case of cutting steel C45.

From the graphs of the radial component of the cutting force F_z , as in Figures 9 and 14, it is shown that the radial component of the cutting force F_z oscillates continuously from the beginning of cutting to the end of the simulation. According to Table 7, the average value of the radial component of the cutting force F_z in the case of cutting the titanium alloy Ti-6Al-4V is 443.2 (N), which is 1.3 times more than the case of cutting steel C45. Thus, according to the formulas (5), (6), (7), the elastic deformation of all elements of the technological system in the case of cutting the titanium alloy Ti-6Al-4V will be 1.3 times greater than in the case of cutting Steel C45 in the same cutting mode. Therefore, the deviations of the diameter of the machined part in the case of cutting the titanium alloy Ti-6Al-4V is greater than in the case of cutting steel C45. In addition, according to the formulas (5), (6), (7), the value of y is the elastic deformation of all elements of the technological cutting system, which changes continuously in the time of cutting due to the oscillation of the radial component of the force F_z with large amplitudes, as in Figure 14. Therefore, the vibration in the case of cutting the titanium alloy Ti-6Al-4V will be greater than in the case of cutting steel C45. The surface quality of the machined parts in the case of cutting the titanium alloy Ti-6Al-4V will be worse than in the case of cutting steel C45.

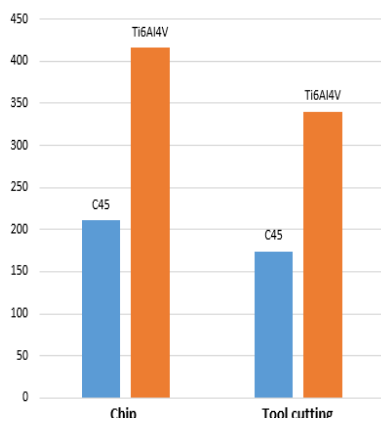


Figure 15. Graph of temperature comparisons on chips and on cutting tools. (° C)

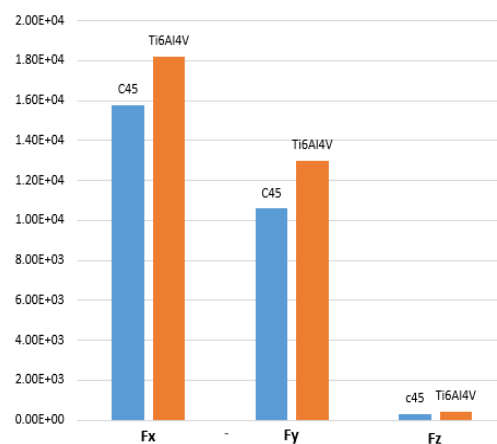


Figure 16. Graph comparing average values of the main component of the force, the feed force and the radial component of the force when machining Steel C45 and titanium alloy Ti-6Al-4V (N.)

5. Conclusions

An orthogonal three-dimensional cutting model is created and the simulation runs. The distribution of the effective stress in the cutting area is considered. The distribution of heat in the cutting area and on the cutting tool is considered. The changes in the components of the cutting forces are considered during the cutting of two materials: steel C45 and titanium alloy Ti-6Al-4V. Analysis and comparison of the obtained simulation results. Specifically, according to the Table 7, Graphs 15, 16 show that all the results obtained from simulations for cutting titanium alloy Ti-6Al-4V are larger than in the case of cutting Steel C45. Therefore, it is shown that the working condition of the cutting tool in the case of cutting the titanium alloy Ti-6Al-4V is harder than in the case of cutting steel C45. The average value of the radial component of the cutting force in the cutting of the titanium alloy Ti-6Al-4V is greater than the case of cutting Steel C45 by 1.3 times. Consequently, the displacements of the cutting head due to elastic deformation in the cutting of titanium alloy Ti-6Al-4V are greater than the case of cutting Steel C45 according to formulas (5), (6), (7), according to which the deviations of the diameter of the machined part will be greater. In addition, the vibration in the cutting increases, the quality of the machined surface of the part deteriorates in the cutting of the titanium alloy Ti-6Al-4V. Hence, the research results show that it is necessary to choose a rational cutting mode, a rational cooling system, a technological system with high rigidity under the actual conditions of cutting the titanium alloy Ti-6Al-4V relative to steel C45.

6. Acknowledgements

The authors are extremely grateful to the anonymous reviewers for their useful comments and suggestions which help to improve the quality of this paper greatly.

References

- [1]. Arshinov V.A, Alekseyev G. A, Rezaniye metallov i rezhurshchiy instrument, Moscow: Mechanical engineering, 1976.
- [2]. Rubinshteyn S.A, Levan G.V, Ornis N.M, Tarasevich YU.S, Rezaniye metallov i rezhurshchiy instrument, Moscow: Mechanical engineering, 1968.
- [3]. Qing Zhang, Song Zhang, Jianfeng Li, "Three dimensional FEM simulation of cutting force and cutting temperature in hard milling of AISI H13 steel," *Procedia Manufacturing* 10, pp. 37-47, 2017.
- [4]. Ran Wang, Tan Luo, Xiaobao Lei, "Finite Element Simulation and Analysis of Stainless Steel 30CrMnSi Orthogonal Cutting," *international conference on mechantronic*, pp. 127-130, 2018.
- [5]. Chechulin YU.V, *Prakticheskoye rukovodstvo k programmnomu kompleksu DEFORM 3D*, Ekaterinburg: URFU, 2010.
- [6]. Hongtao Ding, Yung C. Shin, "A Metallo-Thermomechanically Coupled Analysis of Orthogonal Cutting of AISI1045 Steel," *Journal of Manufacturing Science and Engineering*, vol. 134, pp. 1-12, 2012.
- [7]. DEFORM-3D Material Library..
- [8]. T. O'zel, M. Sima, A.K. Srivastava, B. Kaftanoglu, "Investigations on the effects of multi-layered coated inserts in machining Ti-6Al-4V alloy with experiments and finite element simulations," *CIRP Ann. Manuf. Technol* , vol. 1, no. 59, pp. 77-82, 2010.
- [9]. Cui Chunxiang, Hu BaoMin, Zhao Lichen, Liu Shuangjin, "Titanium alloy production technology, market prospects and industry development," *Materials and Design*, no. 32, pp. 84-169, 2011.
- [10]. Thangavel Jagadesh, G. L. Samuel, "Finite Element Simulations of Micro Turning of Ti-6Al-4V using PCD and Coated Carbide tools," *Journal of The Institution of Engineers*, pp. 5-15, 2017.
- [11]. J. Shi, C. R. Liu, "The influence of material models on finite element simulation of machining," *Journal of Manufacturing Science and Engineering*, vol. 4, no. 126, pp. 849-857, 2004.
- [12]. DEFORMTM 3D User's Manual, V 8.1..
- [13]. Grzegorz Szala, Bogdan Ligaj, "Application of hybrid method in calculation of fatigue life for Steel C45 (1045 steel) structural components," *International Journal of Fatigue*, 2016.
- [14]. S.P.F.C. Jaspers, J.H. Dautzenberg, "Material behaviour in conditions similar to metal cutting: flow stress in the primary shear zone," *Journal of Materials Processing Technology*, no. 122, p. 322-333, 2002.
- [15]. O'zel T, Sima M, Srivastava AK, "Finite Element Simulation of High Speed Machining Ti-6Al-4V Alloy using Modified Material Models," *Transactions of the NAMRI/SME*, no. 38, pp. 1-8, 2010.
- [16]. Gs.Nguyen Dac Loc, Le Van Tien, Ninh Duc Ton, Tran Xuan Viet, *So Tay Cong Nghe Ctm-2, Nxb Khoa Hoc Va Ky Thuat*, 2007.
- [17]. Kostenko G. YU., Tetenko O. V., "Diagnostirovaniye Avtokolebaniy Odnomernogo Protsessa Tocheniya," *Molodoy issledovatel' Dona*, pp. 56-60, 2018.
- [18]. GS. TS. Tran Van Dich, PGS.TS. Nguyen Trong Binh, PGS. TS. Nguyen The Dat, PGS. TS. Nguyen Viet Tiep, PGS. TS. Trần Xuan Viet, *Cong Nghe Che Tao May, NXB Khoa hoc va Ky thuat*, 2003.
- [19]. L. Filice, D. Umbrello, F. Micari and L. Settineri, "On the Finite Element Simulation of Thermal Phenomena in Machining Processes," *Advanced Methods in Material Forming*, pp. 263-278.

Author Profile



Thanh Hung Dao is a lecturer at University of Technology and Education - The University of Danang. From 2004 to 2012, he studied at the faculty of mechanical engineering at Saint Petersburg Polytechnic University in Russia. Interested in the field of computer science, materials and metal cutting process research.